Roller Contact Fatigue Study of Austempered Ductile Iron

V. K. SHARMA

Contact fatigue properties of austempered nodular iron transformed at 230 °C to Rc 45-47 were evaluated using roller contact fatigue tests. At a given load, contact fatigue life of the austempered iron was 35 to 45 pct lower than carburized steel. Shot peening, performed using 1.168-mm diameter Rc 45-55 cast steel balls to Almen strip intensity of 0.006 to 0.008 C, was not beneficial. An increase in the surface compressive residual stress introduced by shot peening was accompanied by surface roughening which lowered the fatigue life by detrimentally influencing the EHD film thickness. Stress induced white etching areas well known to develop in high carbon martensite were found to develop in bainitic microstructure also.

INTRODUCTION

The strength properties of quenched and tempered nodular iron are limited to approximately 690 MPa yield and 900 MPa UTS with less than 2 pct elongation. Austempered nodular iron can provide yield strengths of 690 to 1175 MPa and tensile strengths of 970 to 1590 MPa with sufficient ductility for many critical applications. The properties of austempered nodular iron are greatly influenced by the temperature at which austenite is isothermally transformed to bainite. Depending on the isothermal transformation temperature, basically two types of bainitic nodular irons are presently used commercially. High tensile strength and resistance to abrasive wear are developed when austenite-to-bainite transformation takes place at a relatively low temperature, *i.e.*, 210° to 235 °C. Austempering in the range of 350 to 400 °C is required to obtain maximum ductility and impact properties.

Austempered nodular iron used by GM for automotive rear axle hypoid pinion and ring gear applications is reportedly transformed at 235 °C for two hours. Austenitic-bainitic Kymenite-9805 nodular iron produced by Kymmene Hogfers of Finland is transformed at 350 °C.[1] This iron contains 20 to 50 pct retained austenite and ranges in hardness from Rc 29-35. In contrast, GM's bainitic nodular iron contains less than 10 pct retained austenite and has an apparent hardness of Rc 45-50.

Presently, very limited information on the fatigue properties of austempered ductile iron has been published. Data on the contact fatigue properties is especially sparse. Fatigue properties of the unalloyed iron used by GM for automotive rear axle hypoid pinion and ring gear applications are not available. However, unlike their previously used carburized steel gears, bainitic nodular iron gears at GM are shot peened with strict control in order to obtain comparable bending fatigue life. Fatigue properties of Kymenite-9805 (austenitic-bainitic iron) have been studied in detail by Kymmene Hogfers Foundry.[1] Limited four square gear tests conducted at International Harvester Company confirm excellent properties claimed for the austenitic-bainitic nodular iron. The endurance ratio (fatigue limit in bending/ultimate tensile strength) for ductile iron is shown in Figure 1. The endurance ratios for the austenitic-bainitic iron is significantly higher for equivalent tensile strength quenched and tempered ductile iron. Fatigue limit for various gear materials under Hertzian contact stress is shown in Figure 2. At equivalent hardness, contact fatigue properties of austenitic-bainitic Kymenite-9805 ductile iron are significantly superior to quenched and tempered nodular iron, alloyed

V. K. SHARMA is with Truck Group Engineering International Harvester Company Fort Wayne, IN. Originally presented at the ASM Conference on Austempered Ductile Iron, Chicago, IL, April 2–4, 1984.

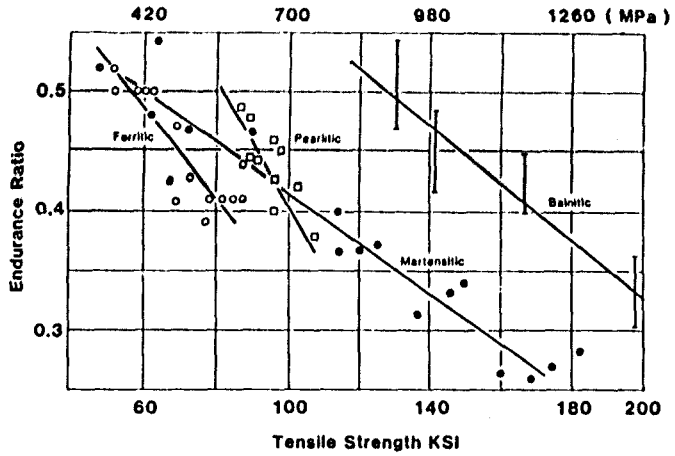

Fig. 1 — Endurance ratio of nodular iron as function of its tensile strength and matrix microstructure. The data for ferritic, pearlitic, and martensitic iron taken from Gray and Ductile Iron Casting Handbook[2]; data for bainitic iron taken from Reference 1.

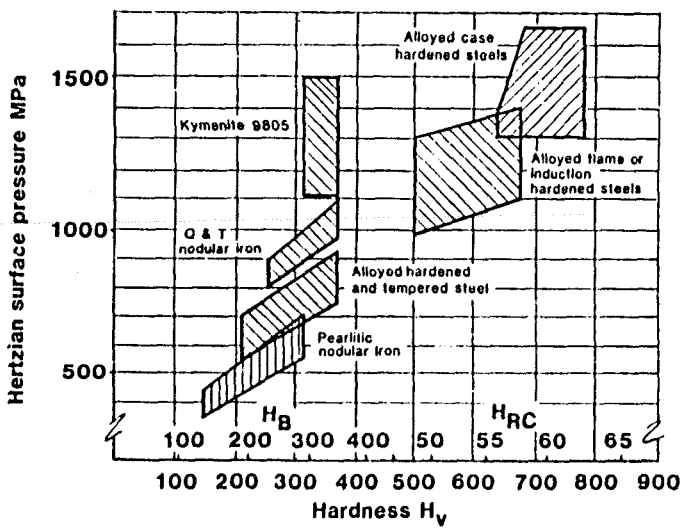

Fig. 2 — Fatigue limit for various materials under Hertzian contact stress.[2]

hardened and tempered steel or pearlitic nodular iron. The properties approach close to much harder alloyed case hardened steels.

Among many failure modes in spur and helical gears, bending fatigue, scuffing, subsurface spalling, and surface pitting have been recognized as the four most frequently encountered. All of these failures are caused by metal fatigue. Although tooth breakage and spalling fatigue are sometimes experienced in heavy duty automotive gearing applications, the gear life is usually limited by surface or near-surface initiated pitting fatigue. To design against pitting, current design practice relies on the stress-life design curves developed by either gear testing or bench tests using a contact specimen which simulates the kinematics and lubrication conditions occurring in gears. Contact fatigue data shown in Figure 2 is useful but it does not provide t' information needed for designing gears. Before austempered nodular iron can be seriously considered for applications involving contact loads, the P-S-N curves for contact fatigue must be developed. The purpose of the present work is to obtain such data and compare the results with well-established stress-life design curves for carburized steel.

TEST EQUIPMENT AND CONDITIONS

The contact fatigue tests were conducted using geared roller test machines. These machines have previously been extensively used to develop materials and evaluate heat treat processes for carburized gears. Our past experience and published information indicates that pit identical to those formed in gears can be produced in these machines under certain sliding conditions.

In the geared roller test machine, a 25.4-mm diameter uncrowned cylindrical test specimen is loaded by a 127-mm diameter load roller which has a 317.5-mm radius crown, see Figure 3. The test arrangement results in a narrow elliptical contact pattern with a minor-to-major axis ratio of 0.11.

The rollers are mounted on two parallel shafts which are supported by double row pressure lubricated bearings. The load is applied to the free end of the upper frame by a calibrated, strain-gaged tension rod through a pneumatically actuated system. The power input is through the lower shaft which contains the test specimen. The upper shaft, carrying the mating roller, is driven by the lower shaft through the phasing gears. Test can be conducted under essentially pure rolling conditions, or negative sliding can be produced on

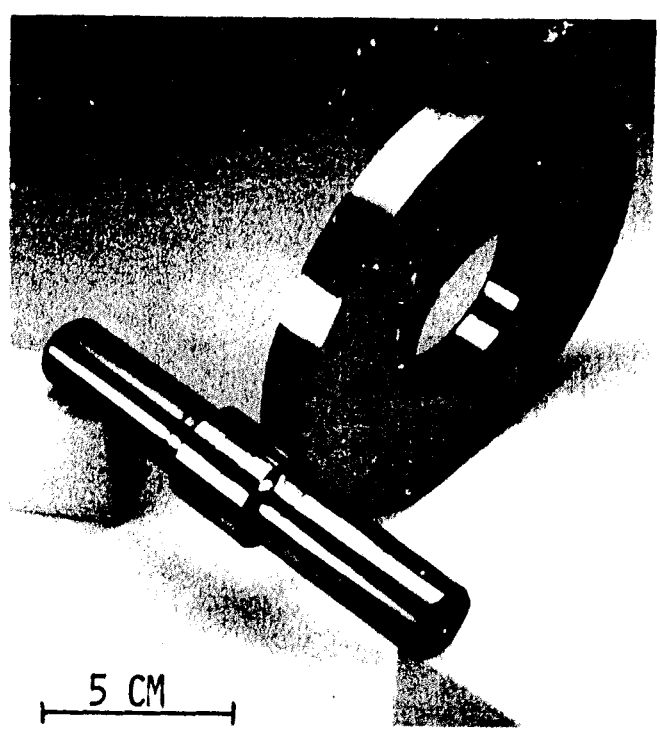

Fig. 3 — Test and load rollers in the geared roller test machine The load roller is 127 mm in diameter and has a 317.5-mm radius crown. The 25.4-mm diameter test roller is not crowned.

the test roller by changing the phasing gear ratio. The test roller is driven at 1330 rpm. Axial movement of the test roller is minimized by compressing a flexible coupling on the shaft containing the test roller.

The test assembly is housed in a controlled temperature oil reservoir. A suitable control system is available to adjust the lubricant sump temperature up to 105 °C. The lubricant is continuously filtered as it is pumped and circulated to the bearings, phasing gears, and test rollers.

Tests were conducted at a calculated Hertz stress ranging from 1240 to 1889 MPa. A phasing gear ratio of 3.5 was used to induce a negative sliding ratio of 0.35 for the test roller. The bulk lubricant temperature was maintained at 85 ± 2.5 °C and was filtered with a 20 μm rated filter. AMOCO multi-purpose gear oil was used as lubricant. Traction coefficient and specimen surface temperatures were not measured because of equipment limitations. Failure was defined as having occurred when a macropit approximately 6 × 5 mm was formed.

MATERIAL AND PROCESSING

SAE ductile iron D-4018 with 0.3 pct Mo and 1.5 pct Ni was used in the studies. Test and mating rollers were machined from sand cast bars or continuous cast bars. Typical composition is given in Table I.

The test surface of the 25.4-mm roller specimen was finish ground to 0.4 μm Ra maximum prior to austempering. The 127-mm diameter load roller had a 317.5 mm crown radius generated on the contact surface after heat treating. Heat treating consisted of austenitizing at 900 °C for 2.5 hours, quenching in 230 °C oil for four hours, and then air cooling to room temperature.

A majority of the test work was performed with the load and the test roller surfaces shot peened to Almen strip intensity of 0.006 to 0.008 C using 1.168-mm diameter Rc 45-55, cast steel balls. The samples had 200 pct shot peening coverage. The surface finish after shot peening was 1.75 to 2.5 μm Ra. Two tests were conducted after grinding the shot peened surface to a surface finish of 0.4 to 0.5 μm Ra. Approximately 0.025-mm deep surface layer was removed diametrically during the grinding process. Additional five tests were performed with the test and load roller surfaces in the as-ground and heat treated condition, having a surface finish of 0.1 to 0.2 μm Ra. Representative pitted rollers were sectioned and metallographically examined to elucidate the mechanism governing contact fatigue in austempered nodular iron.

Table I. Typical Chemical Composition

	Pct		Pct
C:	3.7	P:	0.026
Mn:	0.26	S:	0.009
Si:	2.4	Cr:	0.06
Mo:	0.3	Cu:	0.04
Ni:	1.5	Mg:	0.024

RESULTS AND DISCUSSION

Microstructure

The microstructure of austempered nodular iron is shown in Figure 4. The nodular count in sand cast and continuous cast bars was essentially similar, *i.e.*, 260 nodules per mm^2 and 245 nodules per mm^2, respectively. The microstructure consisted of accicular bainite, retained austenite and nodules of graphite. In addition, all specimens showed small amounts of carbides, martensite and porosity scattered uniformly throughout the microstructure.

Residual stress and the amount of retained austenite were measured on the test surface before and after shot peening using X-ray diffraction techniques. The measurements were performed at the center of the 25.4-mm diameter test area in the circumferential and axial directions. The results given in Table II show that shot peening reduced the amount of retained austenite and introduced significant compressive

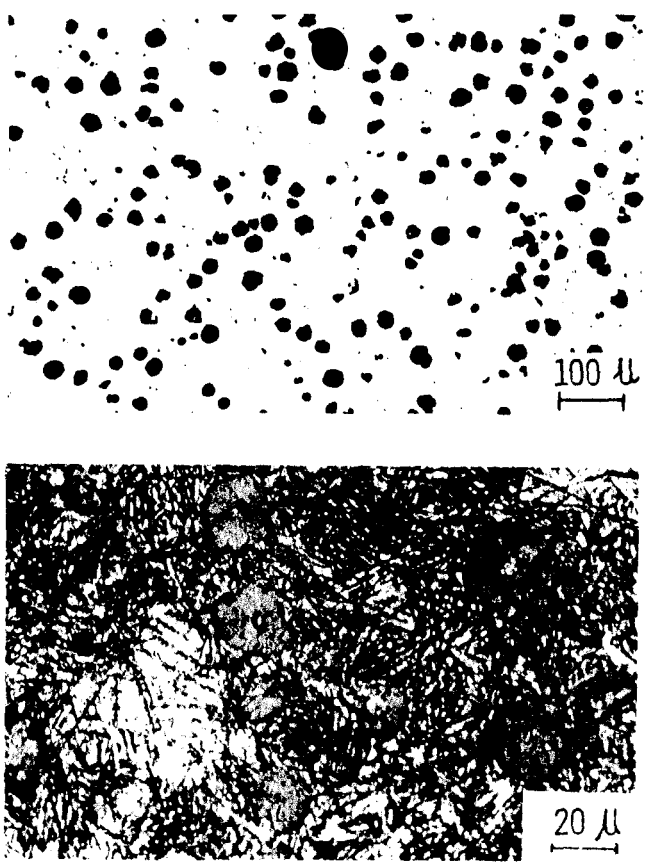

Fig. 4—Microstructures of bainitic nodular iron. Top microstructure unetched; bottom microstructure etched with 2 pct nital.

Table II. Residual Stress And Retained Austenite

Direction 1-in. diameter sample	As Heat Treated RA Pct	As Heat Treated R. stress MPa	Shot Peened RA Pct	Shot Peened R. stress MPa
Circumferential	19	+48	8	−495
longitudinal	19	−62	8	−640

Table III. Typical Tensile Properties

Ultimate:	1485 MPa
Yield:	1205 MPa
Elongation:	1.5 Pct
RA:	2.0 Pct
Hardness:	45.0 Rc

residual stress at the surface. As heat treated surface had tensile residual stress.

Table III shows typical tensile properties. Macrohardness of all test specimens was in the range of 45-47 Rc with a matrix microhardness of 53-56 Rc.

Contact Fatigue

Roller contact fatigue test results (Table IV) are plotted in Figures 5 to 7. The $L50$ curve for carburized steel is included for comparison. The curve for carburized steel is taken from data generated in our laboratory over several years of testing. Notice that the data plotted as load-life curves provide more meaningful comparison of the pitting characteristics of the material than the stress-life (Figure 5) plot. In addition to the load and geometry, the magnitude of contact stress depends on the modulus of elasticity and Poisson's ratio for the two bodies. Because of approximately 30 pct lower modulus of elasticity, for the same load, maximum compressive stress developed in the austempered nodular iron test roller is significantly lower than the stresses developed in carburized steel. The stress-life plot, therefore, inadvertantly tends to underrate the performance of lower modulus materials. Since the primary function of a gear assembly is to transmit load, pitting fatigue behavior of various materials having different modulus of elasticity should be compared on the basis of load-life plots, Figure 6.

A significant amount of wear was observed on all shot peened samples. Typical test tracks are shown in Figure 8. Approximately 0.075-mm deep wear track was formed in shot peened test rollers. When tests were performed after grinding the shot peened surfaces to a surface finish of 0.4 to 0.5 μm or with the test and load roller surfaces in as-ground and heat treated condition (0.1 to 0.2 μm Ra), no significant amount of wear was noticed in the test tracks. Typical surface finishes of test rollers before and after testing are shown in Figure 9. The surface finish of shot peened samples improved from 1.75 to 2.5 μm to 0.6 to 0.8 μm after testing. On the contrary, test surface of as-ground and heat treated samples showed surface roughening. Obviously different lubricating conditions were operative in the two sets of samples.

The results in Figure 7 indicate that, at a given load, contact fatigue life of austempered nodular iron transformed at 230 °C to 45-47 Rc is 35 to 45 pct lower than carburized steel. Shot peening, done as per the specification described

Table IV. Roller Contact Fatigue Test Results

Test No.	Load, Kg.	Cycles in Millions	Roller Surface Condition
A-1	725	3.89	Shot Peened–1.75 to 2.5 μm Ra
A-2	600	5.21	Shot Peened–1.75 to 2.5 μm Ra
A-3	600	5.69	Shot Peened–1.75 to 2.5 μm Ra
A-4	600	8.31	Shot Peened–1.75 to 2.5 μm Ra
A-5	955	1.81	Shot Peened–1.75 to 2.5 μm Ra
A-6	955	1.20	Shot Peened–1.75 to 2.5 μm Ra
A-7	955	1.12	Shot Peened–1.75 to 2.5 μm Ra
A-8	725	3.06	Shot Peened–1.75 to 2.5 μm Ra
A-9	725	3.16	Shot Peened–1.75 to 2.5 μm Ra
A-10	270	>30.01	Shot Peened–1.75 to 2.5 μm Ra
A-11	955	1.72	Peened & Ground–0.4 to 0.5 μm Ra
A-12	600	2.52	Peened & Ground–0.4 to 0.5 μm Ra
B-1	955	1.57	Ground–0.1 to 0.2 μm Ra
B-2	600	11.29	Ground–0.1 to 0.2 μm Ra
B-3	600	5.3	Ground–0.1 to 0.2 μm Ra
B-4	955	1.62	Ground–0.1 to 0.2 μm Ra
B-5	600	11.90	Ground–0.1 to 0.2 μm Ra

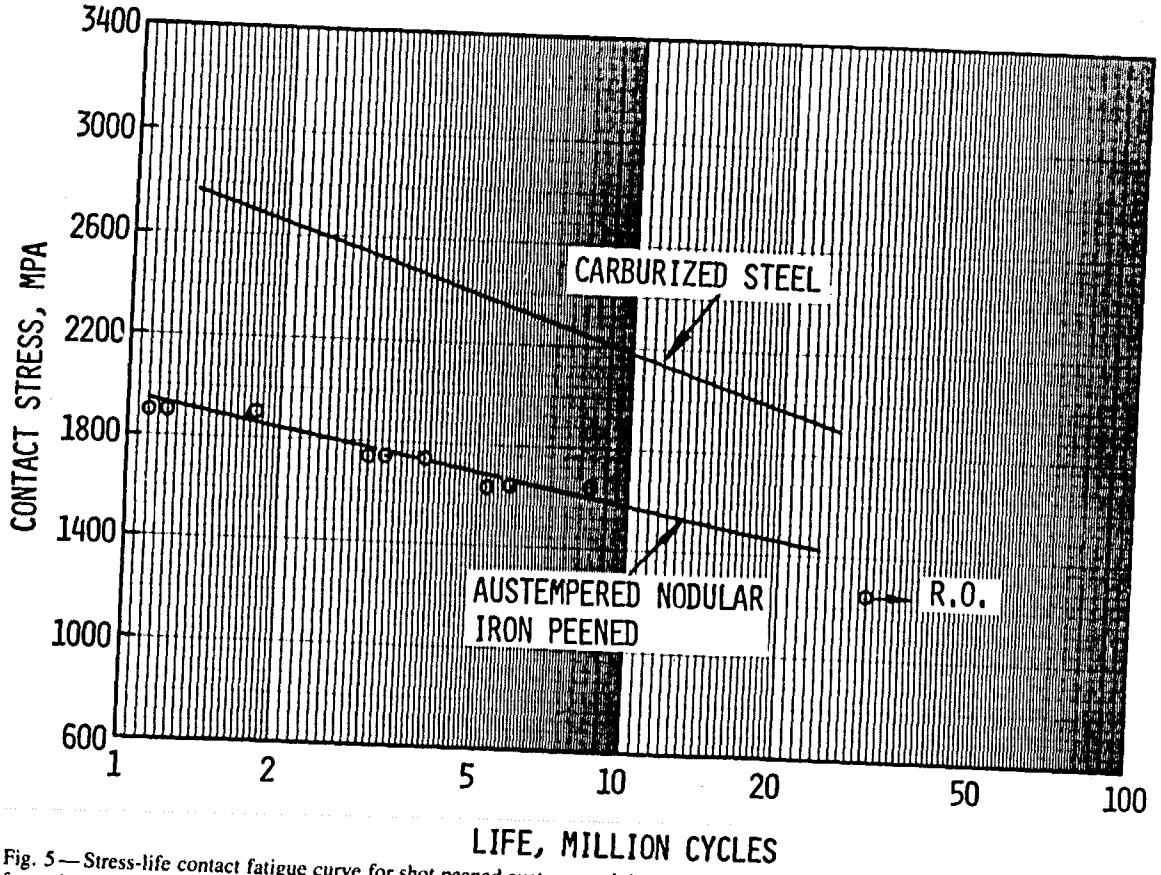

Fig. 5—Stress-life contact fatigue curve for shot peened austempered ductile iron isothermally transformed at 230 °C. L_{50} curve for carburized steel is included for comparison.

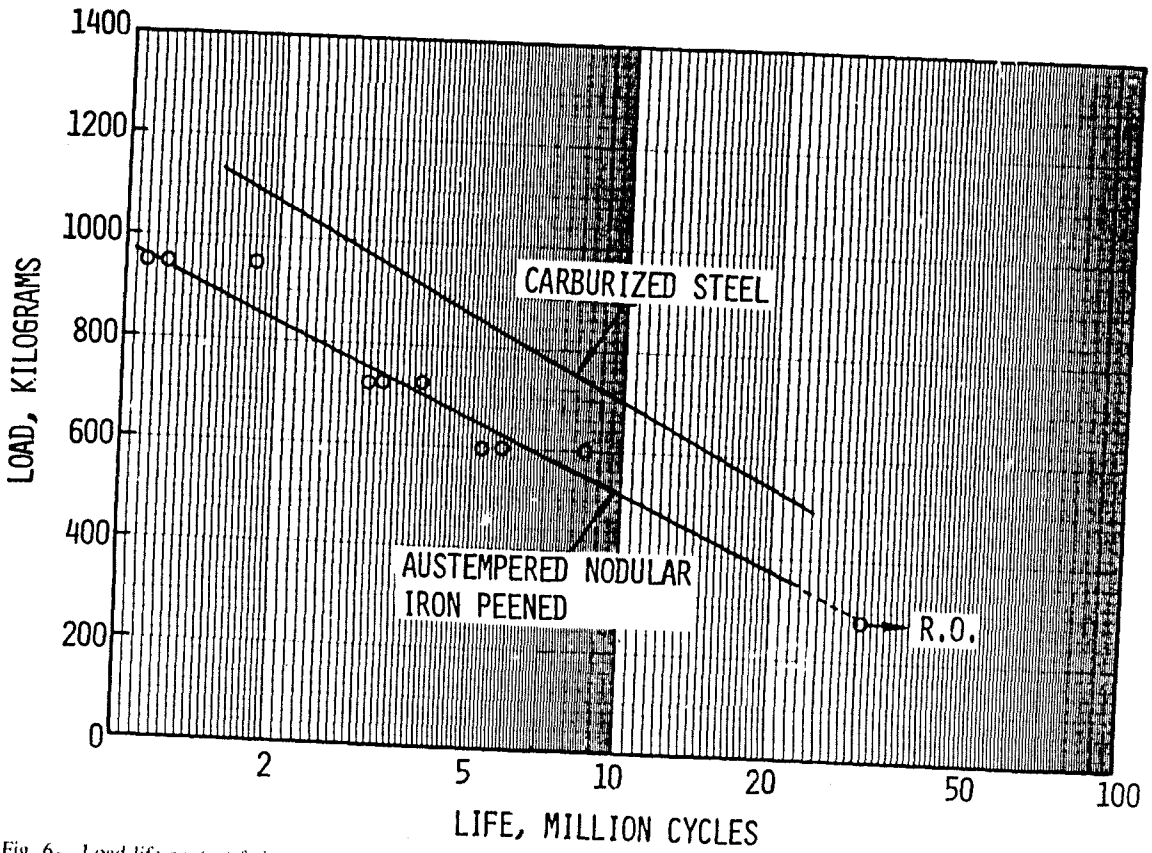

Fig. 6—Load-life contact fatigue curve for shot peened austempered ductile iron isothermally transformed at 230 °C. L_{50} curve for carburized steel is included for comparison.

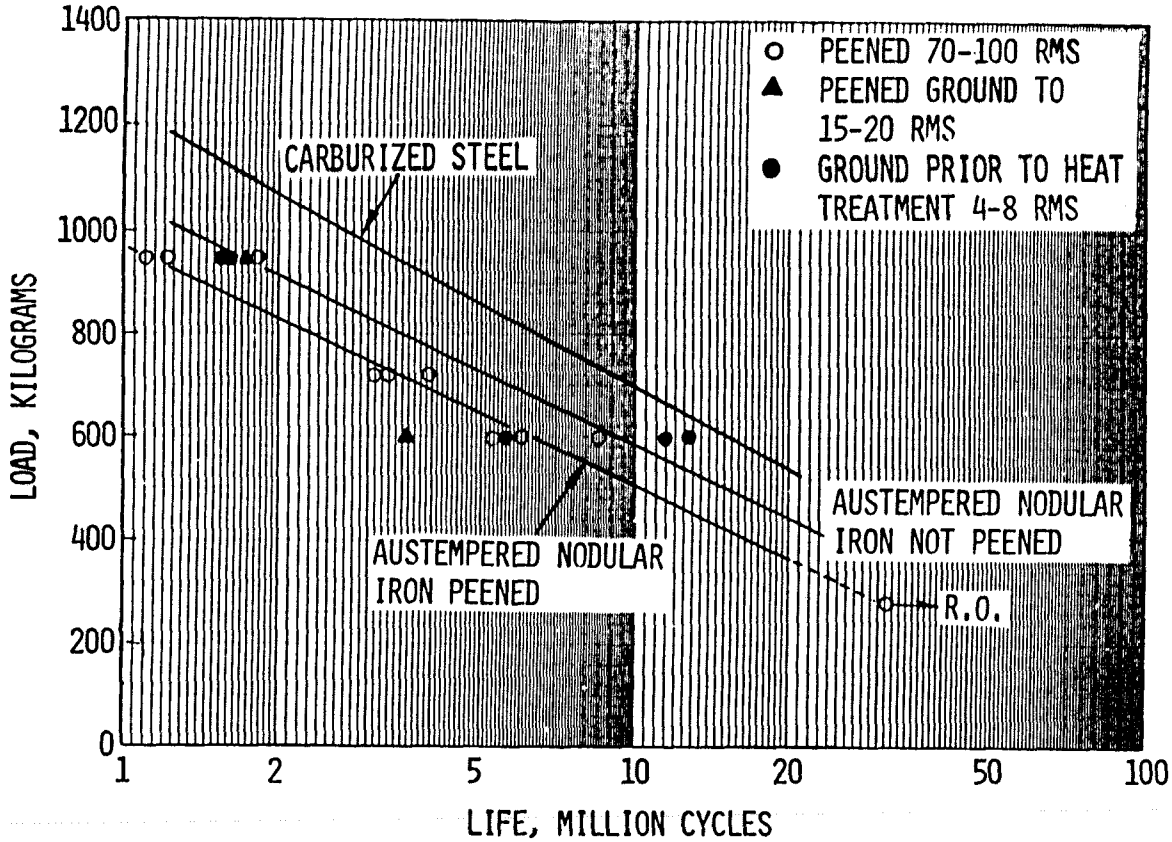

Fig. 7—Load-life contact fatigue curves for austempered ductile iron in as heat treated and shot peened surface conditions. Austempered ductile iron transformed at 230°C. The L_{50} curve for carburized steel is included for comparison.

earlier, was detrimental. It is postulated that an increase in the surface compressive residual stress by shot peening is accompanied by surface roughening which lowers the fatigue life resistance by adversely influencing the EHD film thickness. Obviously, additional work is needed to fully understand the effect of shot peening on contact fatigue properties of bainitic nodular iron. With a proper selection of shot peening parameters, it should be possible to introduce compressive residual stress without significantly damaging the surface such that the net effect will be beneficial. In principal, the presence of compressive residual stresses should retard the initiation and propagation of fatigue cracks and, therefore, improve contact fatigue properties. Sufficient tests were not conducted to determine if the detrimental effect of shot cleaning can be eliminated by grinding the shot peened surface to 0.4 to 0.5 μm Ra.

Pit Formation Process

Although considerable progress has been made in the last two decades toward understanding the mechanism of surface pit formation in gears, it is yet not completely understood. The phenomenon is obviously complex because in addition to the bulk material properties and surface metallurgy, the pitting life is affected by several other factors, including sliding velocity, lubricating conditions, surface roughness, temperature of operation, load magnitude, material impurities, residual stress, etc. The actual failure mode in a given case is a function of the relative detrimental influence of these various factors as they interact with one another.[3] Accordingly, current design approaches for gear systems rely almost exclusively on past practice and empirical approaches.

The results of the present study support findings of a detailed investigation conducted recently at International Harvester and Northwestern University under the sponsorship of NSF.[4,5] The study involved the development of an analytical and phenomenological model to explain the formation of pits in carburized roller test specimens. It was found that transverse microcracks, which eventually propagate to become macropits, are present as early as 5 pct of the total life. Metallographic examination of the microstructure in the microcracked area revealed the presence of a thin (0.8 μm) layer of dark etching microstructural alterations on the surface and a wider band of alterations in the interior. The two dark etching zones were separated by approximately 100-μm thick "quiescent layer" free of microstructural alterations. The dark etching alterations are indicative of the early stage breakdown of martensitic microstructure, which occurs at a threshold cyclic shear stress of about 720 MPa.[6] The presence of a band free of microstructural alterations is indicative of a lower stress

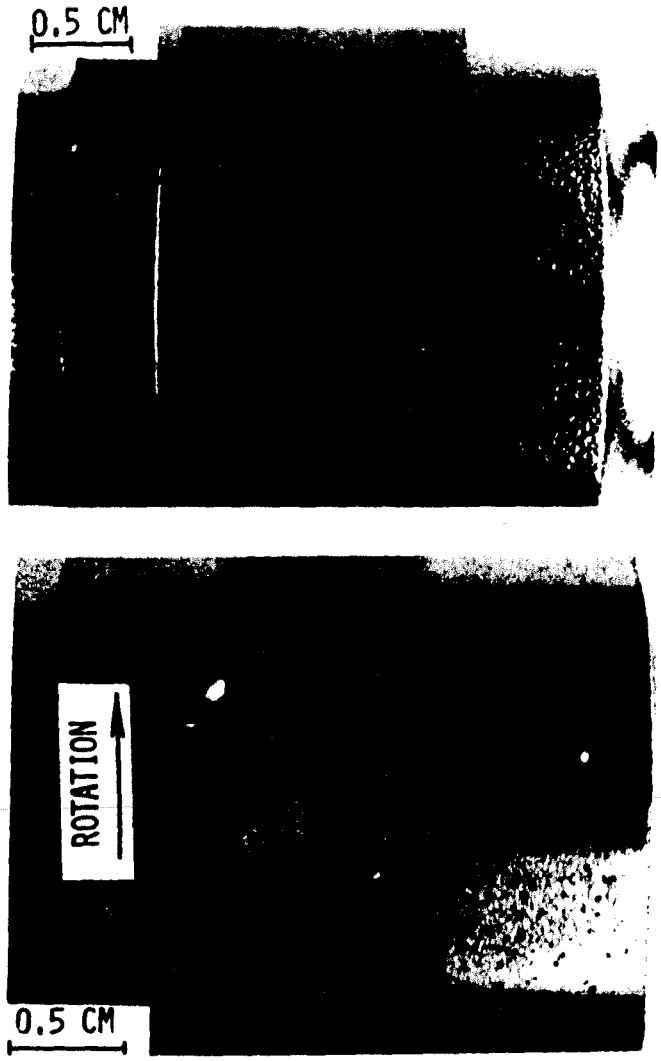

Fig. 8—View of typical test tracks formed in the test rollers. Approximately 0.075-mm deep wear track was formed in the shot peened specimens (top). Rollers with as-ground surface showed no significant wear (bottom).

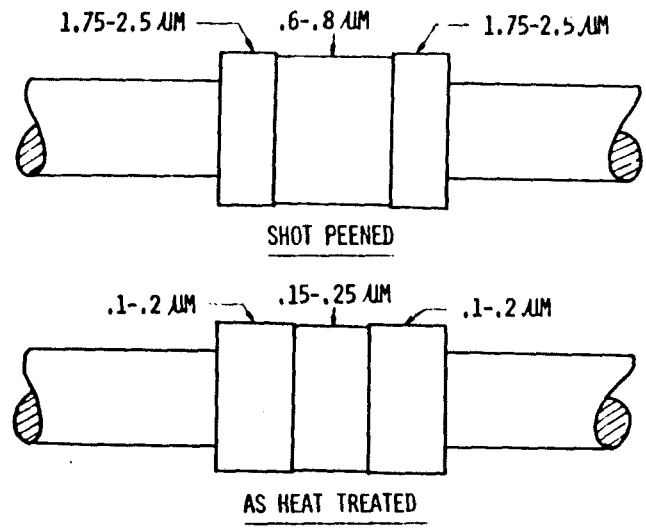

Fig. 9—Typical surface roughness of test rollers before and after testing.

zone postulated by Tallian[3] to explain arrest of surface cracks in contact fatigue. In the NSF study, near-surface non-metallic inclusions were shown to assist the propagation of microcracks from the surface through this "quiescent layer". The microstructural observations were substantiated by analytical stress calculations which included both asperity interactions and bulk stress effects.

Figure 10 shows a typical view of the pit formed in a bainitic nodular iron test roller after 3.06 million cycles at a contact stress of 1730 MPa. Similar to the NSF study on carburized steel, microcracks and micropits were found to form on the test surface early during the tests. These small pits ultimately link together to form a large spall. Selected rollers were sectioned and metallographically examined to further comprehend the pit formation process in bainitic nodular iron. Typical photomicrographs are shown in Figures 11 to 13. With the exception of the microcracks right at the extreme surface (Figure 11), most other cracks were associated with graphite nodules, porosity or dross. Higher stress concentration existing at the edges of non-spherical graphite nodules or defects assist initiation of cracks. These cracks grow to form crack links between the nodules and a pit is formed. Since graphite nodules and other defects serve as sites for primary cracks leading to the pit formation, contact fatigue properties of nodular iron can be expected to be strongly influenced by the nodular count, spheroidicity of graphite nodules and porosity.

Numerous subsurface cracks are developed even when the surface shows no gross macroscopic degradation. Although microcracks were present as much as 350 µm below the surface, the crack density was highest in a narrow band located approximately 175 µm below the surface (Figure 12). This band corresponds to the peak in shear stresses. Unlike the carburized steel rollers, a distinct "quiescent layer" completely free of microcracks was not seen in the bainitic nodular iron test rollers. Lower density of microcracks in a zone starting slightly below the surface to a depth of approximately 175 µm, however, is indicative of a lower stress zone. Similar to the role played by inclusions in carburized steel, graphite nodular or other defects in this area provide a means for linking cracks from the surface to the high shear stress zone. The presence of numerous uniformly distributed graphite nodules throughout the matrix makes it relatively easy for cracks to bridge between the high density subsurface microcrack area and surface. This accounts for the lower contact fatigue properties of austempered nodular iron as compared to carburized steel.

White etching microstructural alterations, geometrically shaped like "butterflies," are well known to develop when high carbon martensitic steel is cyclically stressed under contact loads. These "butterflies" are usually associated with hard oxides, silicate or nitride inclusions. It is generally thought that the "butterflies" do not form around soft manganese sulphide inclusions. These "butterflies" have been

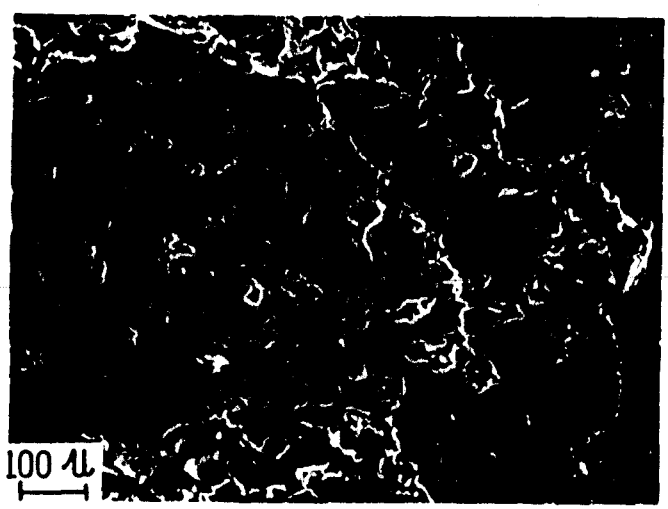

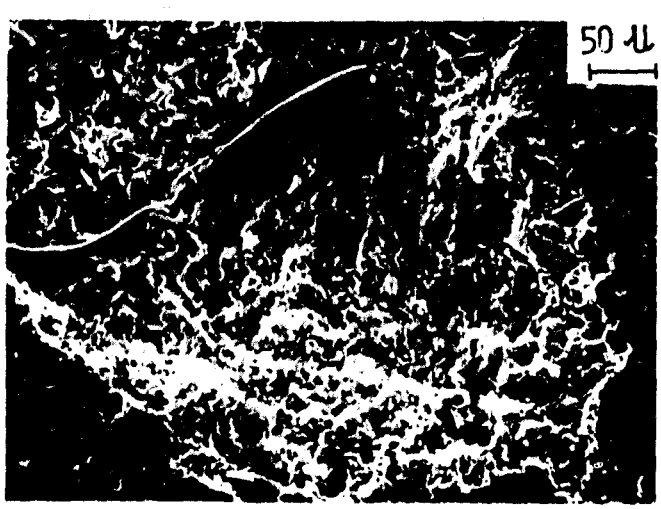

Fig. 10 — Pit formation in bainitic modular iron test roller. Top photomicrograph shows untested shot peened surface. Small pits link together (middle photomicrograph) to form main spall shown in the bottom photomicrograph.

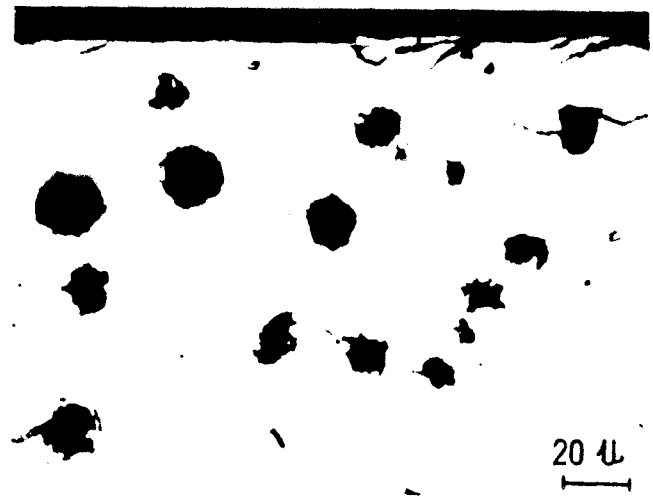

Fig. 11 — Photomicrograph (unetched) shows development of microcracks at and near the surface. With the exception of the microcracks at the extreme surface, all other cracks are associated with nodules or defects.

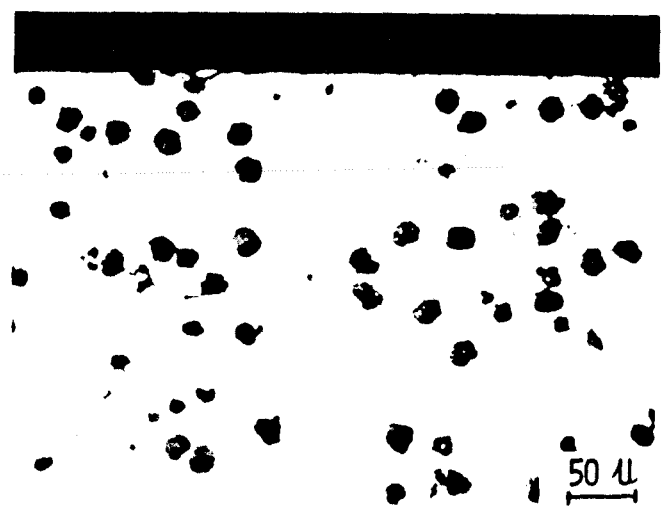

Fig. 12 — Photomicrograph (unetched) shows numerous microcracks concentrated in a band in proximity of the highest shear stresses.

identified to consist of ultrafine grained ferrite and carbide formed as a result of stress-induced transformation of martensite.[7] Figure 13 shows that a similar phenomenon is operative in bainitic nodular iron also. White etching structural alterations were found to form around graphite nodules, carbides, porosity and other high stress concentration sites. Similar to the microcracks (Figure 12), the density of "butterflies" increased in the vicinity of highest shear stress zone. A dark etching region was observed near the extreme surface only. All "butterflies" appear to contain cracks. This tends to confirm the formation mechanism proposed by Becker[7] according to which inclusions in steel contribute to early crack formation which act as severe stress concentration site resulting in a stress-induced transformation of martensite-to-ferrite.

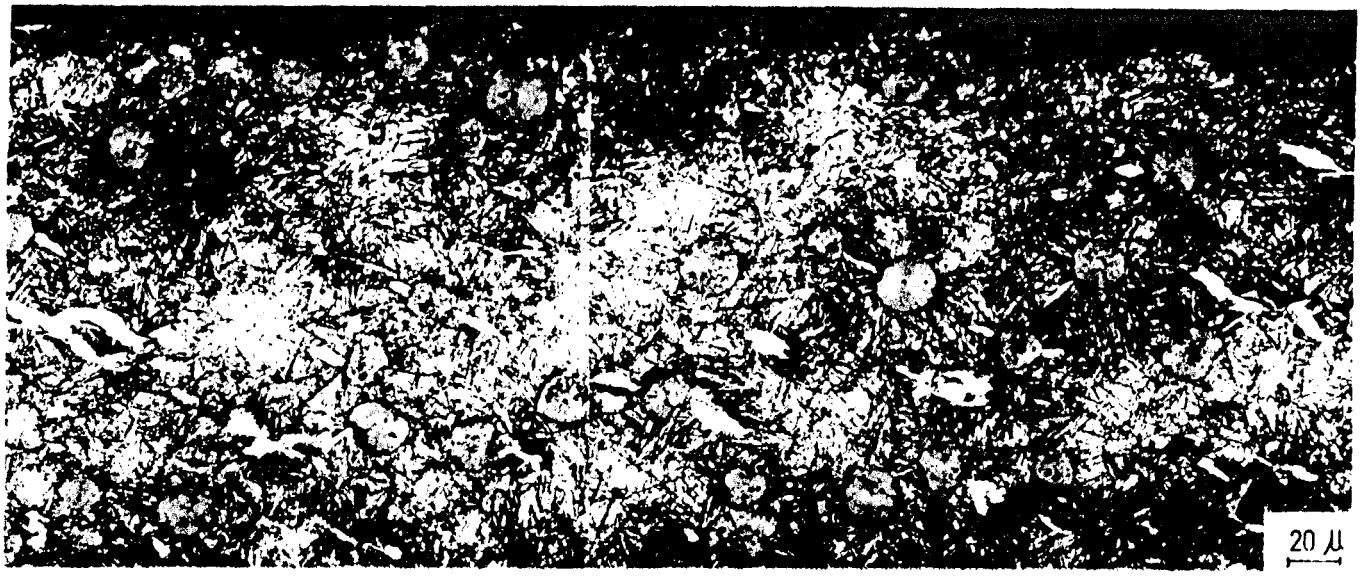

Fig. 13 — Photomicrograph shows white etching "butterflies" formed principally around the nodules in bainitic nodular iron. The density of "butterflies" increased in the vicinity of the highest shear stress zone.

CONCLUSIONS

- At a given load, contact fatigue life of austempered nodular iron austempered at 230 °C to Rc 45-47 is 35 to 45 pct lower than 58-62 Rc carburized steel.
- Shot peening parameters, particularly the shot hardness, must be chosen carefully to avoid excessive surface roughening. Otherwise it can result in reduced contact fatigue by detrimentally influencing the EHD film thickness.
- Contact stress induced white etching microstructural alterations, well known to occur in high carbon martensite around hard oxides, silicates and nitride inclusions, were found to develop in bainitic microstructure also. In austempered nodular iron, white etching "butterflies" are formed around nodules, porosity, dross and other defects.
- Contact fatigue life of austempered nodular iron is strongly influenced by the spheroidicity of graphite nodules, their size and distribution, porosity, and the amount of non-metallic inclusions.
- Additional research and experimentation is needed to develop engineering design data to facilitate rapid and reliable utilization of austempered nodular iron for new engineering applications.

ACKNOWLEDGMENTS

This work was supported by SAE Ad Hoc Ductile Iron Gear Committee. The member companies are acknowledged for their cooperation and support. In particular, I would like to thank Dennis Vukovich, Chairman of the committee, for technical discussions and coordinating this work with the member companies.

REFERENCES

1. M. Johansson: "Austenitic-Bainitic Ductile Iron, *AFS Transactions*, 1977, p. 117.
2. Jokipzz Kalcui: "Isothermal Heat Treated Nodular Iron With Austenitic-Bainitic Microstructure As Material For Gears," *Proceedings of the World Congress on Gearing*, Paris, France, June 1977.
3. T. E. Tallian, Y. P. Chiu, and E. V. Amerongen: "Prediction of Traction and Microgeometry Effects on Rolling Contact Fatigue Life," *Trans. ASME J. Lubric. Technol.*, 1978, vol. 100, no. 2, p. 156.
4. T. M. Clarke, L. M. Keer, T. Mura, N. Yamashita, G. R. Miller, C. S. Wan, V. K. Sharma, and H. S. Cheng: "An Analytical Model for Prediction of Surface Pitting Life in Spur and Helical Gears," Industry/University Cooperative Research submitted by NW University and IH to NSF, September 1983.
5. T. M. Clarke, G. R. Miller, L. M. Keer, and H. S. Cheng: "The Role of Near-Surface Inclusions in the Pitting of Gears," *ASLE Trans.*, 1984, in press.
6. J. A. Martin, S. F. Borgese, A. D. Eberhardt: "Microstructural Alterations of Roller Bearing Steel Undergoing Cyclic Stressing," *J. Basic Eng.*, September 1966, p. 555.
7. P. C. Becker: "Microstructural Changes Around Non-Metallic Inclusions Caused By Rolling Contact Fatigue of Ball-Bearing Steels," *Met. Technol.*, June 1981.